Polymer-coating of photocatalytic particles to prevent sintering in their calcination process

Polymer-coating of photocatalytic particles to prevent sintering in their calcination process

Hikaru Namigata

Kanako Watanabe

Saya Okubo

Daisuke Nagao*

dnagao@tohoku.ac.jp

Department of Chemical Engineering, Tohoku University, 6-6-07 Aoba, Aramaki-aza, Aoba-ku, Sendai, Miyagi, 980-8579, Japan

*Corresponding author.

Abstract

A method to prevent sintering of photocatalytic particles in a calcination process is developed to allow their crystallization without a significant decrease in their specific surface area. A sacrificial layer of polymer to prevent the particle from sintering was employed for the crystallization of amorphous titania particles in the heat treatment at 500 °C. The heat treatment simultaneously removed the polymer layer by pyrolysis. The heat treatment using a sacrificial layer of polymer could suppress a decrease in the specific surface area of titania particles and also maintain colloidal stability in water, attaining a photocatalytic activity higher than that without using a sacrificial layer. These results indicate that the polymer-coating technique is effective for crystallization of photocatalytic particles without a loss of both colloidal stability and photocatalytic activity of the particles.

Abbreviations: TiO_2, titanium dioxide; PSt, polystyrene; TiO_2@PSt, titanium dioxide particles coated with polystyrene shells; TG, thermogravimetric; XRD, X-ray diffraction; MB, methylene blue; DLS, dynamic light scattering; BET, Brunauer-Emmett-Teller

Keywords: Photocatalyst; Titanium dioxide; Polymer coating; Sintering; Aggregation; Colloidal stability

1 Introduction

Photocatalysts exhibiting catalytic activities under light irradiation have received attention as materials to meet modern needs such as water purification and hydrogen production [1–3]. Crystalline titanium dioxide (titania, TiO_2), which has a wide band gap (3.2 eV for anatase, 3.0 eV for rutile [4]), has been a common semiconductor photocatalyst since Fujishima and Honda [5] demonstrated electrochemical photolysis of water using TiO_2 electrodes under ultraviolet light. Because their specific surface areas are much larger than bulk TiO_2, colloidal TiO_2 particles are a promising photocatalyst. TiO_2 photocatalysts have been immobilized on solid stationary supports or dispersed in aqueous solution [6–8]. The former, TiO_2 immobilized on/in a chemically inert layer such as silica gels [9,10] and porous silica [11], has an advantage of easy recovery after photocatalytic reactions. However, photocatalysts immobilized have lower specific surface area exposed to a solution compared to the latter of particulate TiO_2 dispersed in a solution [12]. The high specific surface area of dispersed TiO_2 particles exposed to a solution is expecting to exhibit high rates of photocatalytic reactions [13].

Crystallinity of TiO_2 particles is important for their photocatalytic activities because catalytic activities depend on the degree of the crystallization and the percentage of anatase and rutile phases of TiO_2 particles [14,15]. Recombination of electron-hole sites on atomic defects of TiO_2 particles is restricted by the crystallization, which leads to improvement of their photocatalytic characteristics [16]. Crystallization of amorphous TiO_2 to anatase or rutile can be induced by various methods such as hydrothermal methods [17,18], microwave-assisted hydrothermal methods [19,20] and calcination [21,22]. In particular, calcination is a simple way to crystalize TiO_2 particles at temperatures higher than 300 °C for anatase and 900 °C for rutile, respectively [23]. However, TiO_2 surfaces make contact with each other during the heat treatment, leading to a decrease in the surface areas of the particles due to their aggregation [24,25].

Coating crystalline TiO_2 particles with a layer chemically inert at high temperatures is a possible way to avoid the aggregation of particles in the heat treatment. However, the active sites for photocatalysis on the particles are covered with the inert layer. Porous materials such as zeolite [26] and mesoporous silica [27] are promising layers to cover the particles because the reactants are allowed to be in contact with the catalytic particles through the porous

layers.

An alternative coating of particles has been reported. Okada et al. [28,29] demonstrated that coating particles with thermally stable materials prevented their sintering by calcination. They employed calcium salt as the thermally stable material to prevent direct contact between hydroxyapatite particles. Because the calcium salt layers on the particles were removed by washing with water after the calcination process, the surface of nanoparticles had the composition of crystalline hydroxyapatite.

Here, we propose an alternative method to prevent photocatalytic particles from aggregating during high-temperature calcination. TiO_2 particles coated with a sacrificial layer are crystallized by calcination at 500 °C. Polystyrene (PSt) is chosen as a sacrificial layer because it is thermally decomposed at 350–480 °C [30].The heat treatment in the present method can simultaneously induce crystallization of TiO_2 and remove PSt layers, omitting the washing process for the sacrificial layers. In the present study, the effect of PSt coating of TiO_2 particles on their photocatalytic activities is evaluated. Additionally, the relationship between crystallinity and dispersibility of the calcined particles with PSt layers of different thicknesses is investigated.

2 Experimental section

2.1 Materials

Titanium tetraisopropoxide (TTIP, 95 %), acetonitrile (99.5 %), methylamine aqueous solution (40 wt%), ethanol (99.5 %), dehydrated ethanol (water content <50 ppm), styrene (St 99 %), *p*-styrenesulfonic acid sodium salt (NaSS, 80 %), and potassium persulfate (KPS, 95 %) were purchased from FUJIFILM Wako Pure Chemical Corporation (Osaka, Japan). 3-Methacryloxypropyltrimethoxysilane (MPTMS, 95 %) was obtained from Shin-Etsu Chemical (Tokyo, Japan). The inhibitor for St monomer was removed by an inhibitor removal column. Water was deionized in advance (>18.2 MΩ cm).

2.2 TiO_2 particles coated with thin polymer shells

Submicron-sized TiO_2 particles were synthesized using a sol-gel method with a mixed solvent of ethanol and acetonitrile [23]. Polystyrene (PSt) coating of TiO_2 particles was conducted according to our previous reports [31,32]. TiO_2 particles and a silane coupling agent (MPTMS) were added in a mixed solvent of ethanol and water. After stirring for 1 h at 35 °C, St and NaSS were added to the mixture, and it was stirred for 2 h. The polymerization initiator, KPS, was added to the mixture at 65 °C. TiO_2 particles coated with thin PSt shells (approximately 60 nm) were obtained 12 h after initiation of the polymerization. The PSt-coated particles (TiO_2@PSt-60) were centrifuged at 6000 rpm for 8 min with the reaction mixture. They were subsequently washed twice with water with the same centrifuge conditions. The volume fraction of TiO_2 particles in the mixture was 0.065 vol%. The concentrations of MPTMS, St, NaSS, and KPS were 2.5 mM, 50 mM, 0.25 mM, and 2 mM, respectively.

Increasing polymer shell thickness and calcination of the polymer-coated particles

In order to increase the PSt shell thickness, St monomer was added to the aqueous suspension of the TiO_2@PSt-60 particles (0.05 vol%). After stirring for 2 h at 35 °C, an aqueous solution of KPS was injected into the suspension. The polymerization of St was conducted at 65 °C for 12 h, after which the obtained particles were centrifuged several times with water and ethanol. The concentrations of St and KPS in the process were 100 mM and 2 mM, respectively. TiO_2 particles coated with PSt shells with the other two thicknesses of 180 nm and 270 nm were prepared by repeating the polymerization process. These TiO_2@PSt particles are described as TiO_2@PSt-180 and TiO_2@PSt-270, respectively. The PSt-coated TiO_2 particles were dried under vacuum overnight and calcined at 500 °C for 4 h.

2.3 Evaluation of photocatalytic activities

The photocatalytic activities of TiO_2 particles were evaluated by decomposition of an organic dye (methylene blue, MB) [16]. A suspension of TiO_2 particles was sonicated more than 15 minutes and subsequently mixed with MB aqueous solution. The total volume of the solution was 35 mL, and the concentration of MB added to the aqueous suspension was 16 μM. The solution was stirred for 1 h in the dark (without irradiating UV light) to attain equilibrium of MB adsorption on the surface of TiO_2 particles. After attaining the equilibrium, the initial concentration of MB (C_0) was examined using a calibration curve before light irradiation. UV light (λ = 365 nm, 1.2 mW/cm^2) irradiated the suspension under the continuous stirring for 2 h. Part of the solution (1.5 mL) was taken every 30 min. After centrifuging the suspension in order to separate TiO_2 particles and supernatant solution, absorption spectra of the supernatant were measured with UV-vis spectrometer (Hitachi, U-3900). From the spectra, the residual MB concentrations were determined. A Xe lamp (Asahi Spectra, MAX-303) was employed as the UV source with a band-pass filter (Asahi Spectra, HQBP365-UV φ25) to shield the visible light. The concentrations of TiO_2 particles was 5.0×10^{-2} g/L.

2.4 Characterization

Synthesized particles were observed with a FE-TEM (Hitachi, HD-2700). Size distributions of dispersed particles and zeta potentials were measured with dynamic light scattering (Otsuka Electronics, ELSZ-2). Crystallinity of

the calcined TiO_2 particles was examined with X-ray diffraction (Rigaku, RINT-2200VHF+/PC or Ultima IV). Nitrogen adsorption-desorption isotherms were recorded at −196 °C with BELSORP-mini II (Bel Japan Inc.). The surface areas of the particles were calculated from the adsorption-desorption isotherms with Brunauer-Emmett-Teller (BET) analysis. The volume-averaged diameter (d_V) and the coefficient of variation of particle size distribution (C_V) were determined using the following equations:

$$d_V = \left(\sum n_i d_i^3 / \sum n_i \right)^{1/3}$$

$$C_V = \frac{\left[\sum \{ d_i - (\sum n_i d_i / \sum n_i) \}^2 \right]^{1/2}}{\sum n_i d_i / \sum n_i} \times 100$$

where n_i is the number of particles with diameter d_i. The diameters were determined by measuring more than 200 particle diameters in TEM images. Thermal gravimetric analysis (TGA) was used to examine pyrolysis of polystyrene layers on TiO_2 surfaces. The compositions of the TiO_2 particle surfaces were measured with X-ray photoelectron spectroscopy (XPS).

3 Results and discussion

3.1 Photocatalytic activity of calcined TiO_2 particles pre-coated with polystyrene

A TEM image of amorphous TiO_2 particles synthesized by our previous method is presented in Fig. 1(a). The volume average diameter (d_V) and the polydispersity (C_V) for the particles were 310 nm and 7.9 %, respectively. As shown in Fig. 1(b), spherical particles coated with PSt shells were formed by iterative polymerization of St. Averaged shell thicknesses were estimated by calculating the difference in sizes between TiO_2 cores and PSt-coated particles. In order to crystallize the particles in Fig. 1(a) and (b), they were calcined at 500 °C for 4 h. The calcined TiO_2 particles without PSt layers were non-spherical and the volume of the particles was reduced to approximately 40 % of the volume of the particles before the calcination (see Fig. 1(c)), suggesting that the particles could be densified by the heat treatment. Fig. 1(d) shows the TEM image of TiO_2 particles obtained by calcination of TiO_2@PSt-180. The PSt shells were sufficiently decomposed by heating at around 400 °C according to the TG curve of TiO_2@PSt-180 particles shown in Fig. S1. The calcined TiO_2@PSt-180 particles were as spherical as pristine TiO_2 particles in Fig. 1(a). Based on the TEM images of Fig. 1(b) and (d), the volume of TiO_2 particles obtained by the calcination was 32 % smaller than that without calcination.

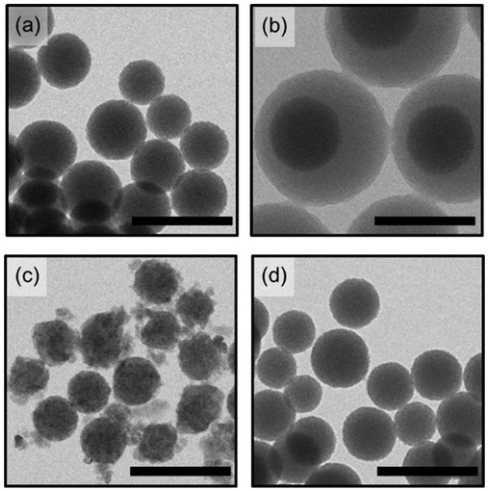

Fig. 1 TEM images of TiO_2 (a) and TiO_2@PSt-180 (b). TEM images of (c) and (d) were particles obtained by calcination of particles (a) and (b), respectively. All scale bars are 500 nm.

alt-text: Fig. 1

Crystallinity of TiO_2 particles is an important factor for discussing the catalytic activities. Fig. 2 presents the X-ray diffraction (XRD) patterns of the calcined TiO_2 particles and TiO_2@PSt-180 particles. According to the XRD patterns, both calcined particles were attributable to anatase phases. The crystallite sizes estimated using Scherrer equation were 28 nm for the calcined TiO_2 and 6.3 nm for the calcined TiO_2@PSt-180, respectively. These results indicate that the crystallization of TiO_2 particles was restrained by the PSt coating.

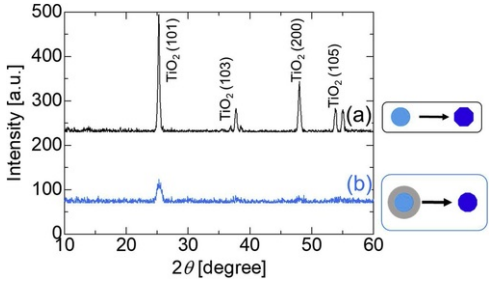

Fig. 2 XRD patterns of the TiO_2 particles (a) and (b) obtained by calcination of TiO_2 and TiO_2@PSt-180, respectively.

alt-text: Fig. 2

Photocatalytic activities of each type of calcined particle presented in Fig. 1(c) and (d) were evaluated using methylene blue (MB). Fig. 3 shows MB concentrations measured in the presence of the calcined TiO_2 or calcined TiO_2@PSt-180 at different irradiation times by UV light. The calcined TiO_2@PSt-180 decomposed MB molecules more rapidly than the calcined TiO_2 particles.

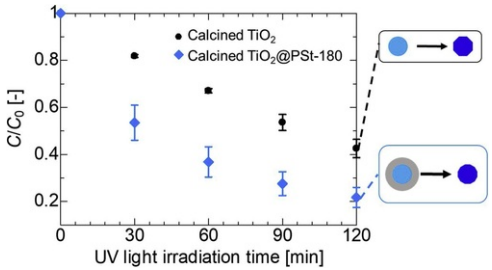

Fig. 3 Photocatalytic activities of the calcined TiO_2 particles (black dots) and the calcined TiO_2@PSt particles (blue rhombuses). (For interpretation of the references to colour in this figure legend, the reader is referred to the web version of this article.)

alt-text: Fig. 3

The difference in the decomposition rate can be explained by the difference in the dispersibility of the calcined TiO_2 particles in water. Fig. 4(a) and (b) show the size distributions of each calcined particle in water measured with dynamic light scattering (DLS). The size distributions of calcined TiO_2 include a peak of particles larger than 1 μm, which is different from the size of the particles observed in Fig. 1(c). A sediment of the particles was not redispersed in water even after sonication for 1 h as shown in Fig. S2, which supported the size distributions measured with DLS. A single peak smaller than 1 μm was observed from the calcined TiO_2@PSt-180 presented in Fig. 4(b), and the particles were dispersed well in water after the calcination. Zeta potentials of the calcined TiO_2 and calcined TiO_2@PSt-180 were -8.5 mV and −38 mV, respectively. The low zeta potential for the calcined TiO_2 particles is probably due to a decrease in the number of hydroxyl groups on surfaces [33,34] caused by direct exposure to high temperature for a long time. The specific surface areas of the particles were calculated using the Brunauer-Emmett-Teller (BET) method in order to investigate the effect on the catalytic activities. A significant difference of the specific surface areas between the calcined TiO_2 and TiO_2@PSt-180 was measured (34 m^2/g and 120 m^2/g, respectively), which indicates that the PSt shells act as a physical barrier to keep the distances between TiO_2 particles during the calcination process.

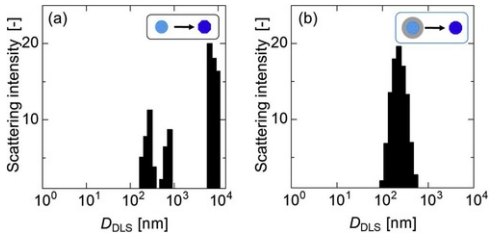

Fig. 4 Size distributions of the calcined TiO_2 particles (a), the calcined TiO_2@PSt particles (b) measured by dynamic light scattering (DLS).

alt-text: Fig. 4

3.2 Effect of polymer shell thickness on photocatalytic activities

TiO_2@PSt particles with different shell thickness (60 nm, 180 nm, and 270 nm) were prepared to investigate the effect of the shell thickness on the photocatalytic activities of the calcined particles. TEM images of the obtained TiO_2@PSt particles are shown in Fig. S3. The PSt-coated TiO_2 particles were calcined at 500 °C, and all the PSt shells were removed from the TiO_2 surfaces (see Figs. S4 and S5). As shown in Fig. S5, there were no difference between the surface of calcined TiO_2 and that of calcined TiO_2@PSt-270. This result indicates that PSt are entirely removed from the surfaces of calcined TiO_2 particles even when the shell is as thick as core.

Fig. 5 describes the C/C_0 of MB at different UV irradiation times for each suspension of the calcined particles. The calcined TiO_2@PSt-60 with the thinnest PSt shells exhibited the lowest catalytic activity among the four samples. Photocatalytic activities higher than TiO_2 particles without PSt shells were attained by coating TiO_2 particles with PSt shells with a thickness of 180 nm or more. The comparison on the variation in MB concentration indicated that the photocatalytic activities depended on the thickness of PSt shell covering the photocatalytic particles (Table S1 shows the rate constants for photocatalytic activity of TiO_2 particles calcined with different shell thickness).

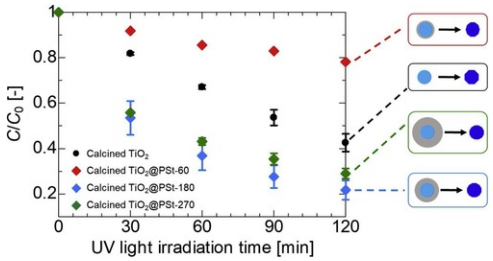

Fig. 5 Photocatalytic activities of the calcined particles. TiO_2 particles (black dots), TiO_2@PSt-60 (red rhombuses), TiO_2@PSt-180 (blue rhombuses), and TiO_2@PSt-270 (green rhombuses). (For interpretation of the references to colour in this figure legend, the reader is referred to the web version of this article.)

alt-text: Fig. 5

The differences in the photocatalytic activities of the calcined particles can be explained by a combination of TiO_2 crystallinity and particle dispersibility in water. The XRD patterns of all the particles are shown in Fig. 6. The peaks of the calcined TiO_2 were attributed to the anatase phase, and the intensity of that was much stronger than the other calcined particles. The estimated crystallite sizes were 5.5 nm for the calcined TiO_2@PSt-60 and 6.3 nm for the calcined TiO_2@PSt-270, respectively.

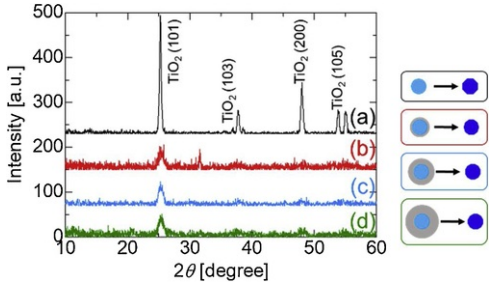

Fig. 6 XRD patterns of calcined particles. TiO_2 particles (a), TiO_2@PSt-60 (b), TiO_2@PSt-180 (c), and TiO_2@PSt-270 (d).

alt-text: Fig. 6

The dispersibilities of the particles, however, exhibited different tendencies between the calcined TiO_2 particles coated with thin shells and thicker shells (see Fig. 7(b)–(d)). Size distributions with particle sizes larger than 1 μm were observed in the case of TiO_2@PSt-60, whereas single peaks of particle sizes smaller than 1 μm was observed in the case of TiO_2@PSt-180 and TiO_2@PSt-270. It is likely that the PSt shells of 60 nm were not thick enough to prevent the particles from aggregating during calcination. The combined results of XRD patterns and size distributions for the calcined particles show that the photocatalytic activities of the TiO_2 particles are dominantly affected by not only their crystallinity but also their dispersibility in water. Both low crystallinity and dispersibility of the TiO_2@PSt-60 caused low photocatalytic activity.

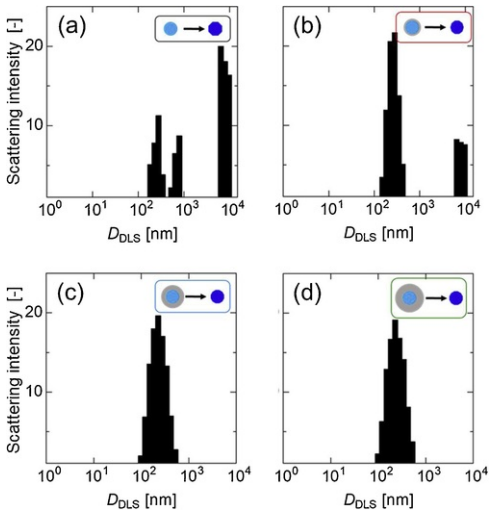

Fig. 7 Size distributions of the calcined particles. TiO_2 particles (a), TiO_2@PSt-60 (b), TiO_2@PSt-180 (c), TiO_2@PSt-270 (d).

alt-text: Fig. 7

According to these results, PSt layers with the thickness of 180 nm or more were effective to prevent the aggregation of submicron-sized TiO_2 particles during the calcination process. PSt layers much thicker than 180 nm, however, suppressed the crystallization of TiO_2 particles. Evidently, coating TiO_2 particles with PSt layers with appropriate thicknesses is important for both their crystallization and avoiding their aggregation in the calcination process.

3.3 Comparison with a commercial photocatalyst of P25

The photocatalytic activity of the TiO_2@PSt-180 that exhibited the highest photocatalytic activities in all samples of Fig. 5 was compared with that of commercial photocatalytic particles of P25. P25, which consists of a mixture of anatase and rutile phases, has a primary particle size of approximately 30 nm and BET surface area of approximately 50 ~~$m^2 g^{-1}$~~ $m^2 g^{-1}$ [9,12,35]. As presented in Fig. 8, the concentration of MB for the calcined TiO_2@PSt-180 was almost the same as that of P25 in the UV irradiation, which suggested the photocatalytic activity of TiO_2@PSt-180 were comparable to P25. Since P25 has high crystallinity but low dispersibility in water (Fig. S6), calcined TiO_2@PSt-180 having high dispersibility in water caused it to exhibit almost the same photocatalytic activity.

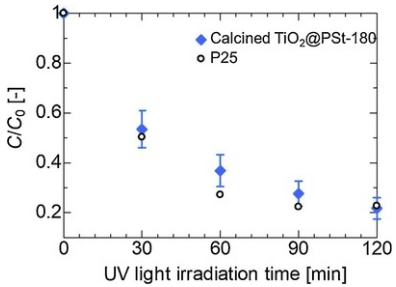

Fig. 8 Photocatalytic activities of P25 and calcined TiO_2@PSt-180.

alt-text: Fig. 8

4 Conclusion

Photocatalytic particles of titania were coated with polymer shells in order to prevent the aggregation of the particles during heat treatment. The polymer-coated titania particles were crystallized from amorphous to anatase phases by calcination at 500 °C. Although the crystallinity of the calcined polymer-coated particles was lower than that of titania particles calcined without polymer layers, the photocatalytic activity of the calcined polymer-coated

particles was much higher than that of the calcined titania particles. The size distribution larger than 1 μm in water was not observed for the calcined particles that were coated with PSt shells thicker than 180 nm. This result indicates that polymer-coating is a practical way to avoid the aggregation of titania particles in the calcination process.

By comparing the photocatalyic activity of our particles with P25, we find that not only the crystallinity of titania particles but also the dispersibility in water are dominant factors for the photocatalytic properties of particles. The proposed approach to coat colloidal particles with a sacrificial layer can be applicable to other particles such as alumina and hydroxyapatite in order to prevent their aggregation by heat treatment.

CRediT authorship contribution statement

Hikaru Namigata: Conceptualization, Validation, Investigation, Writing - original draft. **Kanako Watanabe:** Resources, Writing - review & editing, Supervision, Funding acquisition. **Saya Okubo:** Validation, Investigation. **Daisuke Nagao:** Resources, Writing - review & editing, Supervision, Project administration, Funding acquisition.

Declaration of Competing Interest

The authors declare that they have no known competing financial interests or personal relationships that could have appeared to influence the work reported in this paper.

Acknowledgements

The authors thank technical support staff in the department of Engineering for the measurements, Tohoku University for STEM images. This research was mainly supported by the Ministry of Education, Culture, Sports, Science and Technology (JSPS KAKENHI Grant Numbers 17K19020, 17H02744, 16J03375, 15KK0222).

Appendix A. Supplementary data

Supplementary material related to this article can be found, in the online version, at doi:https://doi.org/10.1016/j.colsurfa.2020.124782.

References

[1] M.R. Hoffmann, S.T. Martin, W. Choi and D.W. Bahnemann, Environmental ~~Applications of Semiconductor P~~applications of semiconductor photocatalysis, *Chem. Rev.* **95**, 1995, 69–96, https://doi.org/10.1021/cr00033a004.

[2] A.L. Linsebigler, G. Lu and J.T. Yates, Photocatalysis on TiO_2 ~~Surfaces: Principles, Mechanisms, and Selected R~~surfaces: principles, mechanisms, and selected results, *Chem. Rev.* **95**, 1995, 735–758, https://doi.org/10.1021/cr00035a013.

[3] K. Hashimoto, H. Irie and A. Fujishima, TiO_{2} ~~photocatalysis: A~~ photocatalysis: a historical overview and future prospects, *J~~apanese J. Appl. Physics,~~pn. J. Appl. Phys. Part 1 Regul. Pap. Short Notes Rev. Pap.* **44**, 2005, 8269–8285, https://doi.org/10.1143/JJAP.44.8269.

[4] M. Nan Chong, B. Jin, C.W. Chow and C. Saint, Recent developments in photocatalytic water treatment technology: ~~A~~a review, *Water Res.* **44**, 2010, 2997–3027, https://doi.org/10.1016/j.watres.2010.02.039.

[5] A. Fujishima and K. Honda, Electrochemical ~~Photolysis of Water at a Semiconductor E~~photolysis of water at a semiconductor electrode, *Nature* **238**, 1972, 38–40, https://doi.org/10.1038/238038a0.

[6] S. Malato, J. Blanco, A. Vidal and C. Richter, Photocatalysis with solar energy at a pilot-plant scale: an overview, *Appl. Catal. B Environ.* **37**, 2002, 1–15, https://doi.org/10.1016/S0926-3373(01)00315-0.

[7] N. Takeda, T. Torimoto, S. Sampath, S. Kuwabata and H. Yoneyama, Effect of inert supports for titanium dioxide loading on enhancement of photodecomposition rate of gaseous propionaldehyde, *J. Phys. Chem.* **99**, 1995, 9986–9991, https://doi.org/10.1021/j100024a047.

[8] H. Yatmaz, C. Wallis and C. Howarth, The spinning disc reactor – studies on a novel TiO_2 photocatalytic reactor, *Chemosphere* **42**, 2001, 397–403, https://doi.org/10.1016/S0045-6535(00)00088-6.

[9] H. Shibata, H. Sakai, P. Rangsunvigit, T. Hirano and M. Abe, Preparation and photocatalytic activity of titania particulate film with silica as binder, *Surf. Coat~~ings Int. Part B Coatings~~. Int. Part B Coat. Trans.* **86**, 2003, 125–130 https://doi.org/10.1007/BF02699623.

[10] H. Chun, W. Yizhong and T. Hongxiao, Preparation and characterization of surface bond-conjugated TiO_2/SiO_2 and photocatalysis for azo dyes, *Appl. Catal. B Environ.* **30**, 2001, 277–285, https://doi.org/10.1016/S0926-3373(00)00237-X.

[11] J. Castañeda-Contreras, V.F. Marañón-Ruiz, R. Chiu-Zárate, H. Pérez-Ladrón De Guevara, R. Rodriguez and C. Michel-Uribe, Photocatalytic activity of erbium-doped TiO_2 nanoparticles immobilized in macro-porous silica films, *Mater. Res. Bull.* **47**, 2012, 290–295, https://doi.org/10.1016/j.materresbull.2011.11.021.

[12] G. Mascolo, R. Comparelli, M.L. Curri, G. Lovecchio, A. Lopez and A. Agostiano, Photocatalytic degradation of methyl red by TiO_2: Ccomparison of the efficiency of immobilized nanoparticles versus conventional suspended catalyst, *J. Hazard. Mater.* **142**, 2007, 130–137, https://doi.org/10.1016/j.jhazmat.2006.07.068.

[13] N. Kieda and T. Tokuhisa, Immobilization of TiO_2 photocatalyst particles on stainless steel substrates by electrolytically deposited Pd and Cu, *J. Ceram. Soc. Japapn.* **114**, 2006, 42–45, https://doi.org/10.2109/jcersj.114.42.

[14] Y. Gao, H. Wang, J. Wu, R. Zhao, Y. Lu and B. Xin, Controlled facile synthesis and photocatalytic activity of ultrafine high crystallinity TiO_2 nanocrystals with tunable anatase/rutile ratios, *Appl. Surf. Sci.* **294**, 2014, 36–41, https://doi.org/10.1016/j.apsusc.2013.12.107.

[15] Y. Tang, S. Fu, K. Zhao, G. Xie and L. Teng, Synthesis of TiO_2 nanofibers with adjustable anatase/rutile ratio from Ti sol and rutile nanoparticles for the degradation of pollutants in wastewater, *Ceram. Int.* **41**, 2015, 13285–13293, https://doi.org/10.1016/j.ceramint.2015.07.111.

[16] K.V. Baiju, S. Shukla, K.S. Sandhya, J. James and K.G.K. Warrier, Photocatalytic activity of sol-gel-derived nanocrystalline titania, *J. Phys. Chem. C* **111**, 2007, 7612–7622, https://doi.org/10.1021/jp070452z.

[17] R.L. Penn and J.F. Banfield, Morphology development and crystal growth in nanocrystalline aggregates under hydrothermal conditions: Iinsights from titania, *Geochim. Cosmochim. Acta* .**63**, 1999, 1549–1557, https://doi.org/10.1016/S0016-7037(99)00037-X.

[18] X. Feng, K. Shankar, O.K. Varghese, M. Paulose, T.J. Latempa and C.A. Grimes, Vertically aligned single crystal TiO_2 nanowire arrays grown directly on transparent conducting oxide coated glass: Ssynthesis details and applications, *Nano Lett.* **8**, 2008, 3781–3786, https://doi.org/10.1021/nl802096a.

[19] J.M. Aquino, R.C. Rocha-Filho, N. Bocchi and S.R. Biaggio, Microwave-assisted crystallization into anatase of amorphous TiO_2 nanotubes electrochemically grown on a Ti substrate, *Mater. Lett.* **126**, 2014, 52–54, https://doi.org/10.1016/j.matlet.2014.04.005.

[20] S. Baldassari, S. Komarneni, E. Mariani and C. Villa, Rapid ~~Microwave-Hydrothermal Synthesis of Anatase Form of Titanium D~~microwave-hydrothermal synthesis of anatase form of titanium dioxide, *J. Am. Ceram. Soc.* **88**, 2005, 3238–3240, https://doi.org/10.1111/j.1551-2916.2005.00562.x.

[21] J.G. Yu, H.G. Yu, B. Cheng, X.J. Zhao, J.C. Yu and W.K. Ho, The ~~Effect of Calcination Temperature on the Surface Microstructure and Photocatalytic Activity of TiO2 Thin Films Prepared by Liquid Phase D~~effect of calcination temperature on the surface microstructure and photocatalytic activity of TiO_2 thin films prepared by liquid phase deposition, *J. Phys. Chem. B* .**107**, 2003, 13871–13879, https://doi.org/10.1021/jp036158y.

[22] D. Fang, Z. Luo, K. Huang and D.C. Lagoudas, Effect of heat treatment on morphology, crystalline structure and photocatalysis properties of TiO_2 nanotubes on Ti substrate and freestanding membrane, *Appl. Surf. Sc.* **257**, 2011, 6451–6461, https://doi.org/10.1016/j.apsusc.2011.02.037.

[23] E. Mine, M. Hirose, D. Nagao, Y. Kobayashi and M. Konno, Synthesis of submicrometer-sized titania spherical particles with a sol-gel method and their application to colloidal photonic crystals, *J. Colloid Interface Sci.* **291**, 2005, 162–168, https://doi.org/10.1016/j.jcis.2005.04.077.

[24] M. Catauro, E. Tranquillo, G. Dal Poggetto, M. Pasquali, A. Dell'Era and S.V. Ciprioti, Influence of the heat treatment on the particles size and on the crystalline phase of TiO_2 synthesized by the sol-gel method, *Materials (Basel)* **11**, 2018, 2364, https://doi.org/10.3390/ma11122364.

[25] C. Su, B.Y. Hong and C.M. Tseng, Sol-gel preparation and photocatalysis of titanium dioxide, *Catal. Today* .**96**, 2004, 119–126, https://doi.org/10.1016/j.cattod.2004.06.132.

[26] Z. Zhang, L. Sun, X. Hu, Y. Zhang, H. Tian and X. Yang, Anti-sintering Pd@silicalite-1 for methane combustion: Eeffects of the moisture and SO2, *Appl. Surf. Sci.* **494**, 2019, 1044–1054, https://doi.org/10.1016/j.apsusc.2019.07.252.

[27] M.A. Lucchini, A. Testino, A. Kambolis, C. Proff and C. Ludwig, Sintering and coking resistant core-shell microporous silica-nickel nanoparticles for CO methanation: Ttowards advanced catalysts production, *Appl. Catal. B Environ.* **182**, 2016, 94–101, https://doi.org/10.1016/j.apcatb.2015.09.012.

[28] M. Okada and T. Furuzono, Fabrication of high-dispersibility nanocrystals of calcined hydroxyapatite, *J. Mater. Sci.* **41**, 2006, 6134–6137, https://doi.org/10.1007/s10853-006-0444-6.

[29] M. Okada, Y. Omori, M. Awata, T. Shirai, N. Matsumoto, S. Takeda and T. Furuzono, Influence of calcination conditions on dispersibility and phase composition of hydroxyapatite crystals calcined with anti-sintering agents, *J. Nanoparticle. Res.* **16**, 2014, https://doi.org/10.1007/s11051-014-2469-0.

[30] K.H. Lee and D.H. Shin, Characteristics of liquid product from the pyrolysis of waste plastic mixture at low and high temperatures: influence of lapse time of reaction, *Waste Manag.* **27**, 2007, 168–176, https://doi.org/10.1016/j.wasman.2005.12.017.

[31] K. Watanabe, D. Nagao, H. Ishii and M. Konno, Rattle-type colloidal crystals composed of spherical hollow particles containing an anisotropic, movable core, *Langmuir* **31**, 2015, 5306–5310, https://doi.org/10.1021/acs.langmuir.5b01148.

[32] K. Watanabe, H. Ishii, M. Konno, A. Imhof, A. Van Blaaderen and D. Nagao, Yolk/shell colloidal crystals incorporating movable cores with their motion controlled by an external electric field, *Langmuir* **33**, 2017, 296–302, https://doi.org/10.1021/acs.langmuir.6b03116.

[33] X. Wang, L. Cao, D. Chen and R.A. Caruso, Engineering of monodisperse mesoporous titania beads for photocatalytic applications, *ACS Appl. Mater. Interfaces* **5**, 2013, 9421–9428, https://doi.org/10.1021/am401867s.

[34] L.T. Zhuravlev, The surface chemistry of amorphous silica. Zhuravlev mSurface Chemistry of Amorphous Silica. Zhuravlev Model, www.elsevier.nl/locate/colsurfa, 2000, (Accessed 6 December 2019).

[35] H. Zheng, H. Svengren, Z. Huang, Z. Yang, X. Zou and M. Johnsson, Hollow titania spheres loaded with noble metal nanoparticles for photocatalytic water oxidation, *Microporous Mesoporous Mater.* **264**, 2018, 147–150, https://doi.org/10.1016/j.micromeso.2018.01.012.

Appendix A. Supplementary data

The following is Supplementary data to this article:

TG curves of the calcined TiO_2@PSt-180 (Fig. S1) and a photo of agglomerates of the calcined TiO_2 (Fig. S2). TEM images of the PSt-coated TiO_2 particles with different PSt thicknesses (Fig. S3), TEM images of the calcined particles (Fig. S4) and XPS patterns of the calcined TiO_2 and the calcined TiO_2@PSt-270 (Fig. S5). XRD patterns of P25 and size distributions of P25 measured by DLS (Fig. S6). The calculation of degradation rate constants of each calcined particle (Table S1).

Multimedia Component 1

Graphical abstract

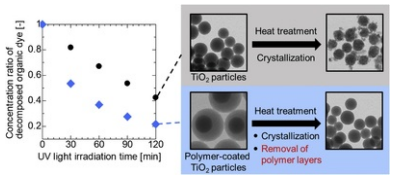

Queries and Answers

Query: Figs. 3 and 5 will appear in black and white in print and in color on the web. Based on this, the respective figure captions have been updated. Please check, and correct if necessary.
Answer: We have checked the updated sentence.

Query: Your article is registered as a regular item and is being processed for inclusion in a regular issue of the journal. If this is NOT correct and your article belongs to a Special Issue/Collection please

contact r.saravanakumar@elsevier.com immediately prior to returning your corrections.

Answer: It is correct that our article belongs to a regular item.

Query: The author names have been tagged as given names and surnames (surnames are highlighted in teal color). Please confirm if they have been identified correctly.

Answer: Yes

Query:

Answer: We confirmed the CRediT authorship contribution statement.

Query: Please check the hierarchy of the section headings.

Answer: The hierarchy is correct.

Query: Have we correctly interpreted the following funding source(s) and country names you cited in your article: Ministry of Education, Culture, Sports, Science and Technology?

Answer: The answer of Q6 is "yes." The funding source of this research is Ministry of Education, Culture, Sports, Science and Technology. However, we would like to ask you to change Acknowledgements as follows (another grand number has been added): The authors thank technical support staff in the department of Engineering for the measurements, Tohoku University for STEM images. This research was mainly supported by the Ministry of Education, Culture, Sports, Science and Technology (Materials Processing Science project ("Materealize") of MEXT, Grant Number JPMXP0219192801 and JSPS KAKENHI Grant Numbers 17K19020, 17H02744, 16J03375, 15KK0222).

Attachments: Acknowledgement.docx